

Magnetic force and optical force sensing with ultrathin silicon resonator

著者	ONO Takahito, Esashi Masayoshi
journal or publication title	Review of scientific instruments
volume	74
number	12
page range	5141-5146
year	2003
URL	http://hdl.handle.net/10097/35175

doi: 10.1063/1.1623627

Magnetic force and optical force sensing with ultrathin silicon resonator

Takahito Ono^{a)}

Graduate School of Engineering, Tohoku University, 01 Aza-aoba, Aramaki, Aobaku,
980-8579 Sendai, Japan

Masayoshi Esashi

New Industry Creation Hatchery Center, Tohoku University, 01 Aza aoba, Aramaki, Aobaku,
980-8579 Sendai, Japan

(Received 21 April 2003; accepted 9 September 2003)

In this article, we demonstrated magnetic and optical force measurements using an ultrathin silicon cantilever down to 20 nm or 50 nm in thickness. The cantilever was heated in an ultrahigh vacuum for enhancing the Q factor and a magnetic particle was mounted at the end of the cantilever using a manipulator. The vibration was measured by a laser Doppler vibrometer and its signal was fed to an opposed metal electrode for electrostatic self-oscillation. An application of a magnetic field with a coil exerted a force to the magnetic material, which results in the change of the resonant frequency. However, the change in the mechanical properties of the cantilever, due to mechanical instability and temperature variation, drifts the resonance peak. Force balancing between the magnetic force and an electrostatic force in the opposite phase can minimize the vibration amplitude. From the electrostatic force at the minimum point, the exerted force can be estimated. A magnetic moment of 4×10^{-20} J/T was measured by this method. The same technique was also applied to measure the optical force of $\sim 10^{-17}$ N, impinging on the cantilever by a laser diode. © 2003 American Institute of Physics. [DOI: 10.1063/1.1623627]

I. INTRODUCTION

A micromachined cantilever has versatile applications for sensing a small force,¹⁻⁶ a mass,⁷⁻⁹ and a surface stress,^{10,11} as widely used in scanning probe microscopy for imaging physical interaction between a sample and a sensor tip.¹² Many approaches have attempted to minimize the noise and raise the sensitivity for advanced sensing, including scaling down,¹³⁻¹⁵ electrical Q control,¹⁶ and mechanical parametric amplification.^{2,17} Among them, the miniaturization of the mechanical sensing elements is a promising method to raise the sensitivity due to its simplicity. In general, a thermomechanical noise limits the sensitivity, which can be suppressed by the scaling down. Recently, various kinds of ultimate sensing have been demonstrated by using micro- or nanomechanical sensors, such as Chacimir force,³ nuclear magnetic resonance (NMR),¹⁸ electrometer for single electron,⁴ etc. Specifically, the application of NMR has been paid great interest owing to its potential ability for the detection of an individual spin and its high resolution imaging, in which a magnetic interaction between a sample and a magnet converts to the mechanical vibration of a mechanical element. Some challenging studies have been conducted for futures quantum computer system based on individual spin detection.¹⁹ Mamin *et al.*¹ had demonstrated sub-aN force detection using a silicon cantilever in a low temperature. However, this interaction force is quite small; despite many efforts, the force sensitivity is still far from the individual spin detection. Another interest in the magnetic force detection is the magnetometry of a small quantity of magnetic

materials based on magnetic torque,^{5,20,21} resonance response in a magnetic field gradient,²² and two-dimensional electron system at the end of a cantilever.²³

In this article, we demonstrate the magnetic force measurement using an extremely sensitive resonating silicon cantilever with a thickness of 20 nm or 50 nm. The small force sensor shows the actual sensitivity of an order of 10^{-16} N/ $\sqrt{\text{Hz}}$. Force balancing between electrostatic and magnetic torque can determine the magnetic moment of a sample. The same method was extended to optical force measurement.

II. EXPERIMENT

Ultrathin cantilever beams made of single-crystalline silicon, with thickness of 50 nm and 20 nm were fabricated by a micromachining technique. The details of the fabrication method are described in Ref. 24. Prior to the measurement, the silicon cantilever was heated at 1000 °C for about 10 s in an ultrahigh vacuum chamber with a pressure of 2×10^{-8} Pa in order to enhance the mechanical quality factor (Q factor).²⁵ The cantilever was heated by flowing a current into the handle wafer supporting the cantilever. The same technique to prepare the high Q cantilever was applied to sensing an adsorbed mass on a subpico-g sample, as described in Ref. 8. To stabilize the mechanical properties, the surface was exposed to atmosphere for oxidizing the surface and reintroduced into the ultrahigh vacuum chamber.

Figure 1 shows the schematic of the measurement system. The cantilever was actuated by applying an ac voltage to a metal electrode situated above the cantilever using a function generator, and the vibration was detected via an

^{a)}Electronic mail: tono@cc.mech.tohoku.ac.jp

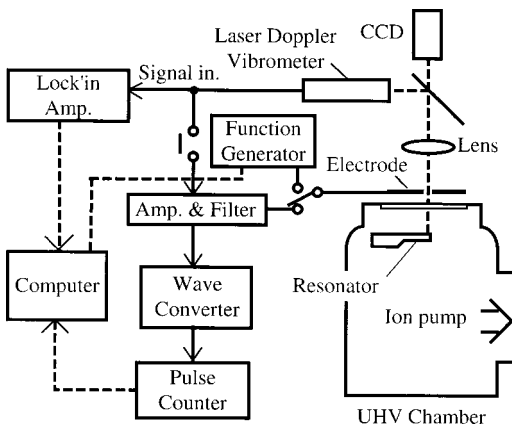


FIG. 1. Schematic of measurement setup.

optical window by a laser Doppler vibrometer with a spot size of $1.5 \mu\text{m}$ and a power of 1 mW. For the self-oscillation of the cantilever, the vibration signal was fed to the electrostatic metal electrode via an amplifier and filter, instead of a pulse generator. The vibration amplitude and the phase were analyzed by a lock-in amplifier, and the frequency was measured by a frequency counter. A computer was employed to control or acquire data from the above instruments via a general purpose interface bus. For magnetometry, a small magnetic particle was mounted on the cantilever by an electrochemically etched tungsten needle with a precisely controlled XYZ stage under an optical microscope.

III. MAGNETIC FORCE SENSING

A. Resonance response of self-oscillated cantilever

The spring constant k of a rectangular cantilever beam is given by $k = Ewt^3/4\ell^3$, where E is Young's modulus, and w , t , and ℓ are the width, the thickness, and the length of the cantilever beam, respectively. The fundamental resonant frequency is given by $f_0 = 0.162t/\ell^2(E/\rho)^{1/2}$. Mass loading, Δm , reduces the frequency to f' , which is given by

$$\Delta m = \frac{k}{4\pi^2} \left(\frac{1}{f'^2} - \frac{1}{f_0^2} \right). \quad (1)$$

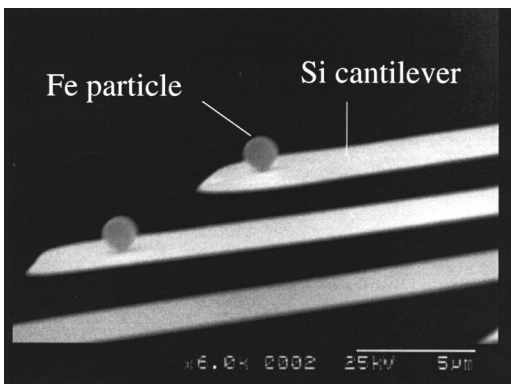


FIG. 2. Typical SEM image of silicon cantilevers on which a Fe particle was mounted.

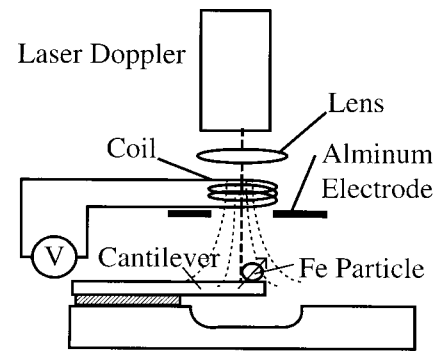


FIG. 3. Schematic illustration of measurement setup for magnetic force measurement based on resonance response by an application of an external magnetic field gradient with a coil.

Ultrathin cantilevers can be used to detect a small force, which minimal noise with a given bandwidth is expressed as follows:

$$F_{\min} = \sqrt{\frac{2k_B T k \Delta \omega_0}{\pi Q \omega_0}}, \quad (2)$$

where k_B is Boltzmann constant, T is the temperature, k is the spring constant, Q is the mechanical Q factor, and ω_0 is the resonant frequency ($\omega_0 = 2\pi f_0$). The presence of a derivative force F' modifies the effective spring constant k_{eff} of a cantilever according to

$$k_{\text{eff}} = k - F'. \quad (3)$$

For F' small compared to k the resonant frequency f' of the cantilever is given by

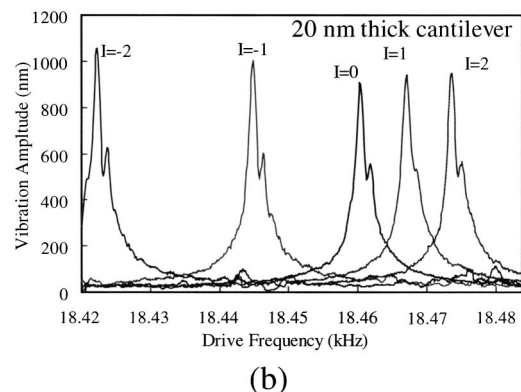
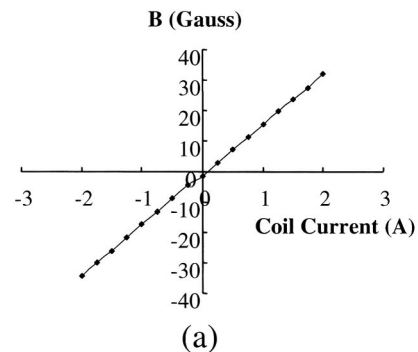


FIG. 4. (a) Relationship of the magnetic field and the coil current at the position of cantilever. (b) Typical resonance spectra under various magnetic fields.

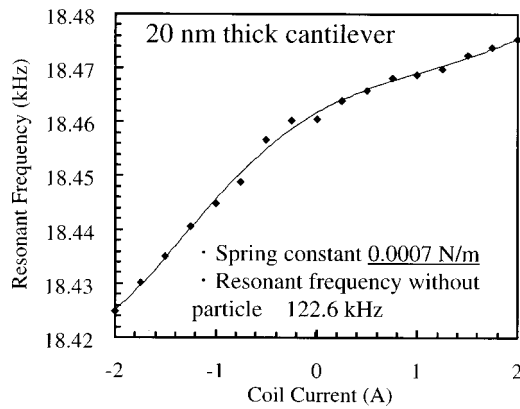


FIG. 5. Resonant frequency changes plotted as a function of the coil current.

$$f' = f_0 \left(1 - \frac{F'}{2k} \right). \tag{4}$$

Next, consider a magnetic interaction between a sample mounted on the cantilever beam and an external magnetic field normal to the plane of the cantilever. If assuming that the sample has a magnetic moment, m_z , along a derivative magnetic field, the force acting on the sample is given by

$$F = m_z (\partial B / \partial z). \tag{5}$$

We get the force gradient F' ,

$$F' = m_z \frac{\partial^2 B}{\partial z^2}. \tag{6}$$

From Eq. (4), this force gradient causes a frequency change.

A 20 nm thick cantilever (the length is 15 μm , the width is 7 μm) was employed to demonstrate magnetic force sensing of an iron (Fe) particle. The cantilever was electrostatically oscillated by applying a voltage of 1.5 V between the electrode and the cantilever, and the vibration amplitude was measured to be about 1 μm at the resonance. The measured resonant frequency (before mass loading) and the estimated spring constant were 122.6 kHz and 0.0007 N/m, respectively. The Q factor of the cantilever was about 20 000. The iron particle with a diameter of about 3 μm was mounted at the end of the cantilever beam, as the typical scanning electron microscopy (SEM) image, is shown in Fig. 2. After the

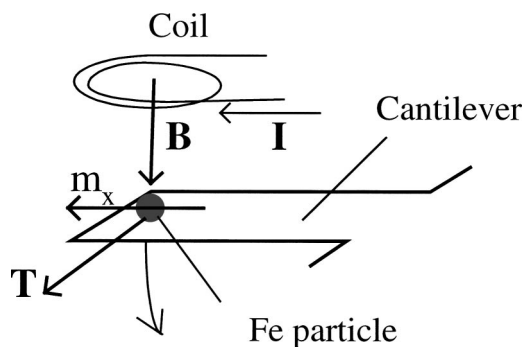


FIG. 6. Schematic figure for magnetic torque vibration.

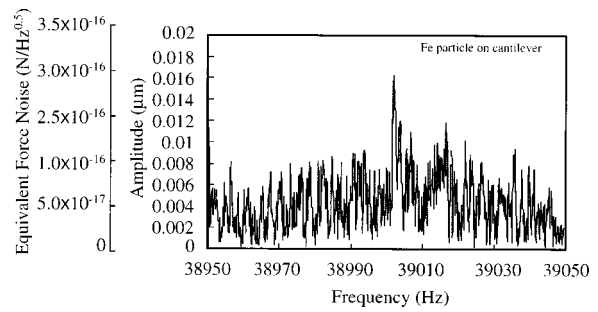


FIG. 7. Noise spectrum density of the Fe-mounted cantilever beam without any external force.

mass loading, the resonant frequency changed to about 18.46 kHz, from which the mass of the iron particle can be estimated to be 5.1×10^{-11} g from Eq. (1).

A coil (50 turns of a copper wire) with a diameter of about 13 mm was placed above the cantilever at a distance of about 8 mm, as shown in Fig. 3. By flowing a current into the coil, the magnetic field gradient can be applied to the iron particle via the optical window. The magnetic field measured by a Hall sensor at the sample position is plotted as a function of the current flowing into the coil in Fig. 4(a). The magnetic field was about 12 Gauss at the sample position with a coil current of 1 A. Figure 4(b) shows the typical resonance spectra, and the resonant frequency change is plotted as a function of the coil current in Fig. 5.

For example, the resonant frequency at 1 A is about 6 Hz higher than that without the magnetic field. According to Eq. (4), this force gradient F' is estimated to be -4.6×10^{-7} N/m, which corresponds to the force of 4.6×10^{-13} N. The detectable frequency change was 0.01 Hz with this cantilever using a measurement setup; therefore, the resolution of the force gradient is to be 8×10^{-10} N/m. If the correct value of $\partial^2 B / \partial z^2$ is known, the magnetic moment, m_z , can be derived from Eq. (6). By using a known magnetized sample as a reference, the magnetic moment will be estimated.

B. Measurement of magnetic torque

With a 50 nm thick (111)-oriented cantilever (4 μm thick, 9 μm wide, 38 μm long), a magnetic torque force loaded on a 1.5 μm diameter Fe particle was measured. The Fe particle on the cantilever was magnetized along to the cantilever direction by applying a dc magnetic field of 0.6 T using an electromagnet. The resonant frequencies of the can-

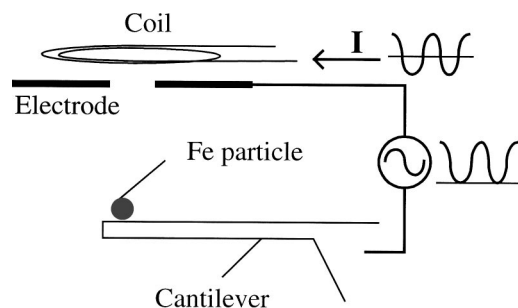


FIG. 8. Schematic illustration of the force balancing between electrostatic and magnetic forces.

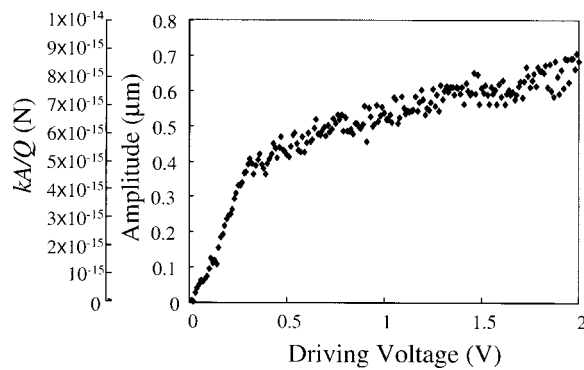


FIG. 9. Vibration amplitude as a function of driving voltage for electrostatic actuation.

tilever beam before and after mass loading were 46 014 Hz and 33 977 Hz, respectively. From the frequency change, the mass of the Fe particle was estimated to be 1.3×10^{-11} g. It should be noted that the Q factors of the cantilever beam before and after the mass loading were 70 000 and 12 000, respectively.

Under an external magnetic field \mathbf{B} , a torque \mathbf{T} acting on the magnetic moment \mathbf{m} is given by

$$\mathbf{T} = \mathbf{m} \times \mathbf{B}. \quad (7)$$

The component of magnetic moment parallel to the cantilever causes the bending of the cantilever, as shown in Fig. 6. In the fact, an ac magnetic field: $B = B_{ac} \cos \omega t$ was applied to the cantilever and the vibration amplitude caused by the magnetic torque was measured by the laser Doppler vibrometer. Figure 7 shows the vibration noise of the cantilever mounted on the Fe particle near the resonant peak without any external force, and the equivalent force noise kA/Q (where A is the amplitude) is indicated in the vertical axis. Although the estimated force noise from Eq. (2) is 1.2×10^{-17} N/ $\sqrt{\text{Hz}}$, the maximal force noise at the resonance was about 3×10^{-16} N/ $\sqrt{\text{Hz}}$, which is indicating that the dominated noise source is not dominated by the thermomechanical noise of the cantilever. This measurement system is not installed an isolation vibration system, therefore, a background vibration noise from ambient seems to limit the minimal detectable force.

Generally, a force is detected by measuring the mechanical response of a cantilever under an application of periodic

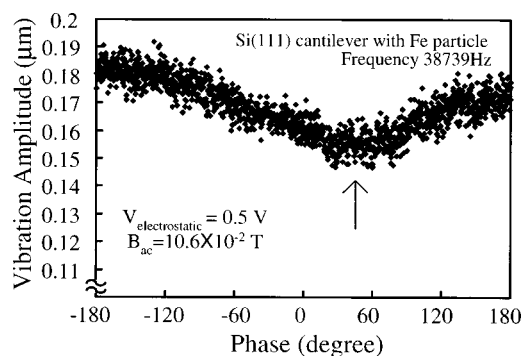


FIG. 10. Vibration amplitude vs phase between driving ac voltage and coil ac current. At the phase of 45° , electrostatic force and magnetic force was in the opposite phase.

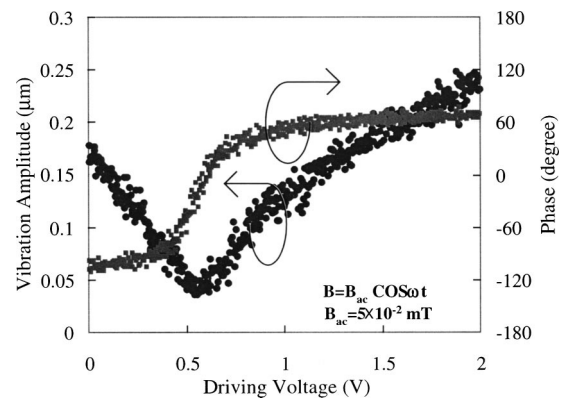


FIG. 11. The magnetic force of 5×10^{-2} mT and electrostatic force was balanced at the driving voltage of 0.57 V.

force. However, mechanical characteristics influence this response in this method. Nonlinearity of the spring and drift of the resonance frequency make the quantitative measurements from the amplitude difficult. In this ultrathin cantilever beam, a hard spring effect often appears and causes the measurement errors.

In this experiment, two external forces were applied to cantilever beam at the same frequency as shown in Fig. 8, and the vibration amplitude was measured as changing the phase or driving the voltage for electrostatic actuation. The electrostatic force is generated by applying an ac voltage between the cantilever and the electrode situated above the cantilever at a distance of about 6 mm. The vibration amplitude and corresponding equivalent force of the cantilever, when only the electrostatic force was applied, was plotted as a function of the amplitude of driving voltage that was fixed at the resonance frequency, as shown in Fig. 9. However, the nonlinear spring effect make this evaluation of force difficult at large amplitudes $> 0.3 \mu\text{m}$, where the obtained curve is not proportional to electrostatic force $\sim V^2$.

Figure 10 shows the vibration amplitude as a function of phase between the magnetic and the electrostatic driving voltage, which exhibits a minimal value at the phase $\sim 45^\circ$, where the electrostatic driving force is opposite in direction to the magnetic force at the minimal point. The equivalent electrostatic force-to-magnetic driving force can be estimated from an amplitude curve in which the driving voltage is

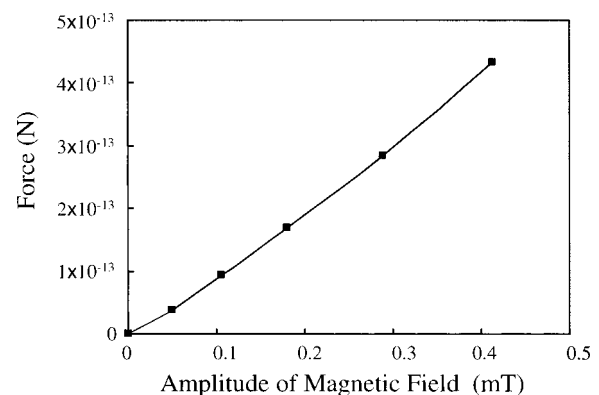


FIG. 12. Observed relationship of the magnetic force and the amplitude of magnetic field.

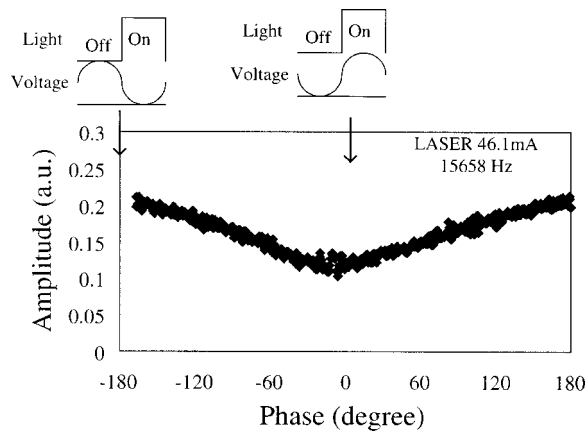


FIG. 13. Amplitude vs phase between the optical pulse signal and the electrostatic driving voltage.

gradually increased at phase=45°, as the typical curve is shown in Fig. 11. This measurement was performed at an external magnetic field of 0.10 mT. The driving voltage showing a minimal value in amplitude was 0.57 V, of which the force can be considered to be same as the magnetic force. Roughly estimated electrostatic force loading on the cantilever at 0.57 V is 1.0×10^{-13} N. The measured driving forces, F_{electro} , under various magnetic fields are plotted in Fig. 12. The force is almost proportional to the external magnetic field. This result is consistent with Eq. (7). The magnetic moment parallel to the cantilever is calculated to be 3.9×10^{-20} (J/T) by $m_z = F_{\text{electro}} \times \ell / B_{\text{ac}}$, which corresponds to a moment per atom of $2.3 \pm 0.2 \mu_B$, where $\ell = 35 \mu\text{m}$ is the length from the fixing point of cantilever to the Fe particle. Within the error, this corresponds to the known bulk value of Fe of $2.2 \mu_B$ at 300 K.

IV. OPTICAL FORCE SENSING

It is known that laser irradiation can generate mechanical force due to light pressure,²⁶ local heating, and photoinduced stress.^{27,28} The measurement of optical force driven by a laser diode was demonstrated by the same technique with magnetic torque sensing as described above. A laser pulse with a spot size of $100 \times 300 \mu\text{m}^2$, wavelength $\ell = 680 \text{ nm}$, impinging on the cantilever (50 nm thick, $4 \mu\text{m}$ wide, $63 \mu\text{m}$ long) at an incident angle of 60°. Figure 13 shows the vibration amplitude in changing the phase between the laser pulse and driving voltage, which shows minimum value at phase

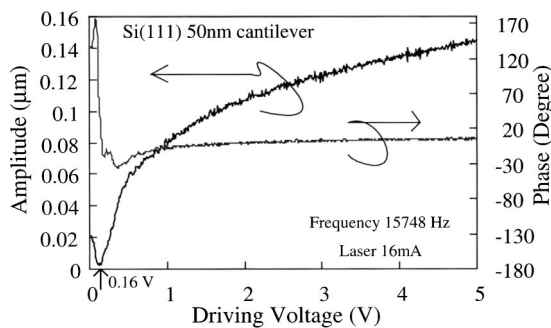


FIG. 14. Amplitude plotted as a function of the electrostatic driving voltage.

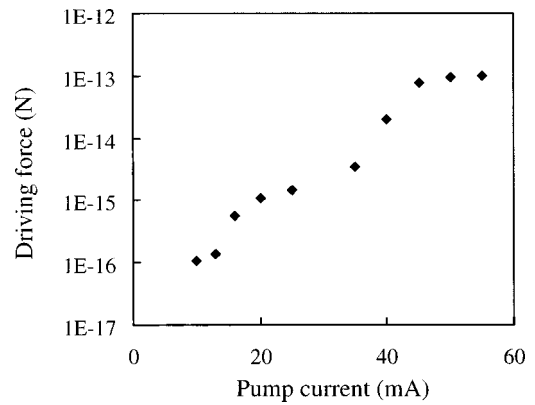


FIG. 15. The measured optical force plotted as a function of pumping current for the laser diode.

~0. The electrostatic driving force is opposite in direction to the optical force at the minimum point, and the phase difference between the optical force and the electrostatic force is almost 180° as well. Figure 14 shows the relation of the vibration amplitude versus driving voltage, measured at phase=0. This measurement was performed at a total laser power range of 10–30 mW and, considering the laser power impinging on the cantilever, is roughly estimated to be 0.2 mW. The driving voltage showing a minimum amplitude at 0.16 V is considered to be same amplitude as the optical force. Roughly estimated electrostatic force loading on the cantilever is 3.7×10^{-17} N. The measured driving forces in various pumping current are plotted in Fig. 15.

V. DISCUSSION

In this article, a magnetic force loaded on a Fe particle with a weight of about ten pico-g situated at the end of an ultrathin cantilever was measured. 50 nm thick or 20 nm thick single crystalline silicon cantilevers were employed for these measurements. The annealed cantilever showed high a Q factor of above 10 000, and the detected force noise was $3 \times 10^{-16} \text{ N}/\sqrt{\text{Hz}}$ after loading the mass. The resonant response under an external magnetic field gradient showed the potential ability of a detectable minimum force of 4.6×10^{-13} N. The large amplitude of vibration causes a mechanical nonlinear effect in sensing. Using two kinds of reciprocal forces can cancel the vibration amplitude, and the nonlinear effects can be minimized. Using this approach, the measurement of the magnetic moment of a Fe particle with a diameter of 1.5 μm was demonstrated. The same technique was extended to measure a light force impinging onto the cantilever. It is expected that this approach can be extended to other sensing for an extremely small force.

ACKNOWLEDGMENTS

This work is supported in part by the Grant-in-Aid for Scientific Research from Ministry of Education, Science, Sports, and Culture of Japan (Grant Nos. 13305010, 12131201, and 14702023). A part of this work was performed at the Venture Business Laboratory, Tohoku University.

- ¹H. J. Mamin and D. Rugar, Appl. Phys. Lett. **79**, 3358 (2001).
- ²A. Dana, F. Ho, and Y. Yamamoto, Appl. Phys. Lett. **72**, 1152 (1998).
- ³H. B. Chan, V. A. Aksyuk, R. N. Kleiman, D. J. Bishop, and F. Capasso, Science **291**, 1941 (2001).
- ⁴R. H. Blick, A. Erbe, H. Krömmmer, A. Kraus, and J. P. Kotthaus, Physica E (Amsterdam) **6**, 821 (2000).
- ⁵C. Rossel, P. Bauer, D. Zech, J. Hofer, M. Willemin, and H. Keller, J. Appl. Phys. **79**, 8166 (1996).
- ⁶P. Mohanty, D. A. Harrington, and M. L. Roukes, Physica B **284**, 2143 (2000).
- ⁷B. Llic, D. Czaplewski, H. G. Craighead, P. Neuzil, C. Campagnolo, and C. Batt, Appl. Phys. Lett. **77**, 450 (2000).
- ⁸T. Ono, X. Li, H. Miyashita, and M. Esashi, Rev. Sci. Instrum. **74**, 1240 (2003).
- ⁹J. P. Cleveland, S. Manne, D. Bocek, and P. K. Hansma, Rev. Sci. Instrum. **64**, 403 (1993).
- ¹⁰M. Godin, V. T. Cossa, P. Grütter, and P. Williams, Appl. Phys. Lett. **79**, 551 (2001).
- ¹¹S. Cherian and T. Thundat, Appl. Phys. Lett. **80**, 2219 (2002).
- ¹²D. Sarid, *Scanning Force Microscopy With Applications to Electric, Magnetic, and Atomic Forces* (Oxford University Press, New York, 1994).
- ¹³P. Mohanty, D. A. Harrington, K. L. Ekinci, Y. T. Yang, M. J. Murphy, and M. L. Roukes, Phys. Rev. B **66**, 085416 (2002).
- ¹⁴K. Y. Yasumura, T. D. Stowe, E. M. Chow, T. Pfafman, T. W. Kenny, B. C. Stipe, and D. Rugar, J. Microelectromech. Syst. **9**, 117 (2000).
- ¹⁵J. Yang, T. Ono, and M. Esashi, J. Microelectromech. Syst. **11**, 775 (2002).
- ¹⁶A. Mehta, S. Cherian, D. Hedden, and T. Thundat, Appl. Phys. Lett. **78**, 1637 (2001).
- ¹⁷D. Rugar and P. Grütter, Phys. Rev. Lett. **67**, 699 (1991).
- ¹⁸D. Rugar, C. S. Yannoni, and J. A. Sidles, Nature (London) **360**, 563 (1992).
- ¹⁹T. D. Ladd, J. R. Goldman, F. Yamaguchi, Y. Yamamoto, E. Abe, and K. M. Itoh, Phys. Rev. Lett. **89**, 017901 (2002).
- ²⁰J. Brugger, M. Despont, C. Rossel, H. Rothuizen, P. Vettiger, and M. Willemin, Sens. Actuators **73**, 235 (1999).
- ²¹T. Höpfl, D. Sander, H. Höche, and J. Kirschner, Rev. Sci. Instrum. **72**, 1495 (2001).
- ²²E. Finot, T. Thundat, E. Lesniewska, and J. P. Goudonnet, Ultramicroscopy **86**, 175 (2001).
- ²³M. P. Schwarz, D. Grundler, I. Meinel, C. Heyn, and D. Heitmann, Appl. Phys. Lett. **76**, 3564 (2000).
- ²⁴X. X. Li, T. Ono, R. Lin, and M. Esashi, Microelectron. Eng. **65**, 1 (2003).
- ²⁵J. Yang, T. Ono, and M. Esashi, Appl. Phys. Lett. **77**, 3860 (2000).
- ²⁶O. Marti, A. Ruf, M. Hipp, H. Bielefeldt, J. Colchero, and J. Mlynek, Ultramicroscopy **42**, 345 (1992).
- ²⁷H. Yu, Y. Wang, C. Ding, Y. Wang, and Y. Xu, Sens. Actuators **77**, 187 (1999).
- ²⁸P. G. Datskos, S. Rajic, and I. Datskou, Appl. Phys. Lett. **73**, 2319 (1998).